

# Toy model for complex behavior of a unicellular organism

Mariana Araújo (n.76284)<sup>1</sup>

<sup>1</sup>*Departamento de Física, Instituto Superior Técnico, Universidade de Lisboa, Lisboa, Portugal*

Unicellular beings such as *Physarum* display the ability for intelligent behaviour despite their simple nature. In this paper, we define a model based on a cellular automaton that simulates such a being. It is capable of achieving its self-sustainability but also its capacity for movement and complex behaviour. Using the model, we obtain simulations for amoebic motion, which include the elimination of potentially harmful structures, such as tentacles and bubble chambers. Additionally, we reproduce the formation and subsequent relaxation of adaptive networks around food sources observed in *Physarum*.

## I. INTRODUCTION

*Physarum* is a unicellular system capable of solving complex problems, including finding the shortest path through a maze and solving the Steiner tree problem, which requires the shortest possible network interconnecting  $n$  points in the plane (for more information on the Steiner tree problem, see [1]). It does so by eliminating redundant paths from all possible paths. This ability is non-trivial: *Physarum* has been shown to be capable of recreating real transport networks such as that of the Hokkaido region of Japan [2]. Unicellular beings such as *Physarum* are composed of a cytoplasmic interior surrounded by a boundary, where the cytoskeleton is concentrated and hardened. Motion is achieved by extending pseudopodia, with cytoplasm flowing to fill them. The flow is guided by the formation of actin filaments inside the cell, in sol-gel conversion reactions. The cohesion of the cell is assured by the reorganization of the cell's components, so that the cytoskeleton once again forms a solid boundary [3].

Amoebic motion has been approached in several studies, although few attempts have been made to connect it with a mechanism for network formation ([4], [5], [6]). More in the vein of this article, previous cell models using cellular automata have been proposed. However, these tend to focus on the self-sustainability of the cell, based on the stable bonding of the components of the cell membrane. In these conditions, the cells obtained tend towards an oval shape and never form a network.

The computing capacity of unicellular beings is intimately tied to the way their movement takes place, and therefore a study that approaches such a connection is of definite importance. In this paper, we use the model of [3] to define amoebic motion for a self-sustainable cell in such a way that it is also capable of forming an adaptive network. We do this by giving up the constraint of strong bonding of the components of the membrane. Instead, we allow for localized softening of the membrane in order to take in external matter, which is transported through the interior of the cell and eventually deposited, resulting in sustainable shape modification.

## II. MODEL

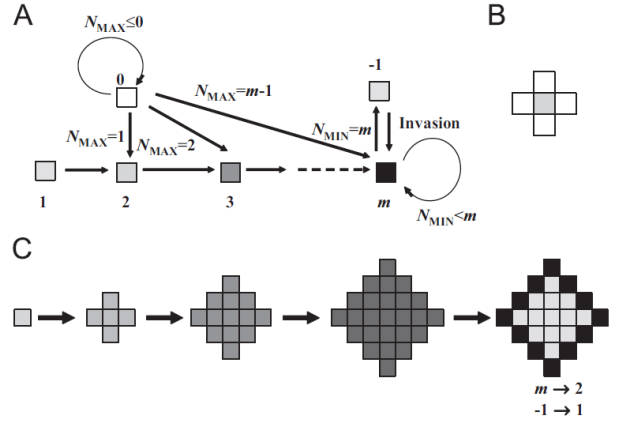


FIG. 1: (A) Transition rule for the development phase. The state of a site is labelled by the integer near it. An arrow indicates a transition.  $N_{max}$  and  $N_{min}$  are the maximum and minimum states, respectively, of the site and its neighbourhood; (B) Neighbourhood of the shaded site; (C) Development of a cell from a seed as described in the text. From [3].

We model a cell by a cellular automaton defined on a planar lattice. The neighbourhood of a site is defined as the four sites directly adjacent to it (see FIG. 1B).

The model has two phases: the development phase and the foraging phase. The former consists of establishing an aggregation of cell components from an initial seed. We initialize all sites of the lattice in state 0, except for the seed, at the centre of the lattice, which has state 1. Then we apply the transition rule of FIG. 1A: the seed and its neighbourhood are set to state 2, then all sites in state 2 and their neighbourhood are set to state 3, etc. This process is repeated until there is a diamond-shaped aggregation of sites in state  $m$ . Then all sites whose neighbourhood is entirely in state  $m$  (the interior of the cell) are set to state -1. In order to simplify further calculations, we redefine the state of the boundary as state 2 and the state of the interior as state 1. The development phase is illustrated in FIG. 1C.

In the foraging phase, the movement of the cell is modelled by an “eating 0” process in which a bubble (state 0) enters the cell due to softening of the membrane and

travels inside it, either being expelled or depositing in its interior. Afterwards, the cell components are reorganized in order to regain its configuration of cytoplasm surrounded by a hardened membrane. The algorithm for the “eating 0” process is the following:

1. Choose a random site with state 2, called the stimulus point (SP);
2. Randomly take one of the neighbours of the SP with state 0. Exchange the state of this neighbour with that of the SP. The state 0 that invades the cell is called a bubble;
3. Set all sites in state 1 to state 2. Set the move counter to 0;
4. Mark the site in which the bubble is located;
5. If the bubble has 3 or more neighbours in state 0, go to step 8. Otherwise, go to step 6;
6. If the move counter exceeds the threshold  $n$ , go to step 8. Otherwise, go to step 7;
7. Randomly choose one of the bubble’s neighbours which is unmarked and in state 2. Exchange the state of the neighbour with that of the bubble. Increase the move counter by 1. If there are no neighbors in this condition, the bubble does not move and the move counter is set to  $n + 1$ . Go to step 4;
8. Set all sites with  $N_{\min} = 2$  to state 1.

The process is illustrated in FIG. 2. This model satisfies the main properties of a cell: it is composed of a mass of cytoplasm surrounded by a membrane; the membrane contains hardened cytoskeleton (both satisfied by the development phase); once the membrane is locally softened, the cytoplasm rushes to the softened part, leading to shape modification and cell locomotion; this movement is accompanied by transportation of the cytoskeleton, whose distribution is then reorganized to enclose the cytoplasm (both satisfied by the foraging phase).

The model has two parameters:  $m$ , which defines the number of cell components  $N = m^2 + (m - 1)^2$ , and the moving time limitation of a bubble  $n$ . For the study of amoebic motion, we consider  $m = 8$  and  $n = 200$ . To study adaptive networks, the cell distribution is defined beforehand: we set  $N = 400$  and  $n = 500$ .

The definition of the model requires one final ingredient: cells will move in the direction of a nutrient gradient and therefore, in order to reproduce this characteristic in our model, we introduce active zones, from which bubbles enter the cell preferentially, to represent food sources.



FIG. 2: The “eating 0” process: A SP, from which a bubble enters, is randomly chosen; All sites of the cell are set to state 2; The bubble traverses the cell and is eventually ejected; The cell’s components are reorganized. Time passes from left to right and from top to bottom. The bubble’s path as it moves through the cell is coloured grey for easier comprehension.

### III. RESULTS AND DISCUSSION

#### A. Amoebic motion

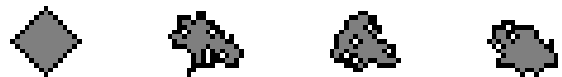


FIG. 3: Evolution of a cell as the “eating 0” process is iterated. Sites are colored black, grey or white if they are in state 2, 1 or 0, respectively. Time passes from left to right. Several iterations are performed between consecutive images.

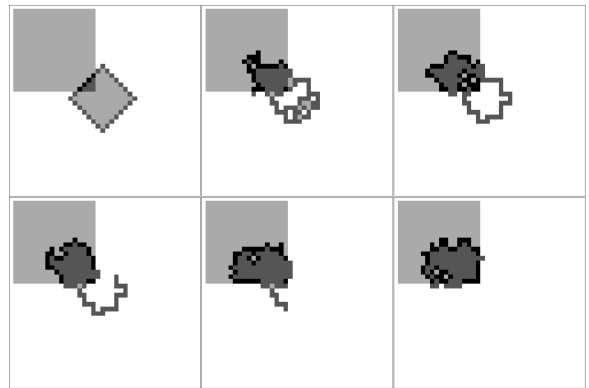


FIG. 4: Evolution of a cell in the presence of an active zone, defined as the shaded region in the upper left corner of the array. Time passes from left to right and from top to bottom. The last image is obtained after 900 iterations.

When the “eating 0” process without active zones is applied repeatedly, we observe a deformation of the cell’s boundary upon each iteration but an overall conservation of shape and position, as can be observed in FIG. 3.

In the presence of active zones, the cell moves in their direction, reproducing the migration of cells to nutrient sources. The movement can be observed in FIG. 4, where an active zone is defined in the upper left corner of the array.

We observe that as the cell moves, bubbles are concentrated in its bottom right, forming a chamber which eventually bursts and creates a tentacle (thin structure of sites in state 2). The tentacle shrinks until the cell is once again stable and in an oval shape. These events, which lead to conservation of cell shape, are due to the joint action of steps 4 and 7 of the algorithm, determining that a bubble cannot retrace its movement. This property, called memorized flow, is also responsible for the deposition of bubbles inside the cell. The mechanisms behind these consequences of memorized flow are simple: when a bubble enters the cell through the boundary of a bubble chamber, then it must travel along it to the body of the cell. If it reenters the boundary through another connection with the body of the cell, then it will move until it reaches the SP. Since it has traversed both the sites ahead of it and the sites behind it, it has nowhere to move and deposits, forming a hole in the chamber's boundary which effectively bursts it. If a cell has a tentacle and a bubble, on its path through the cell, enters the structure, then its only available direction of movement is toward the end of the tentacle. Once it reaches this point, there is no possibility of movement and it deposits, shortening the tentacle length. Finally, a bubble may travel in such a way that its previous path blocks it off from the boundary of the cell. Once it has traversed all sites available to it, it cannot move in any direction and deposits in the cell's interior.



FIG. 5: Consequences of memorized flow. Time passes from left to right. (A) A bubble enters through the border of a bubble chamber and bursts it; (B) A bubble traverses a tentacle, shortening it; (C) A bubble is trapped by its previous path and deposited in the cell.

The events described are illustrated in FIG. 5. Although bubbles can be deposited in the cell in this way, its stability is preserved. Without this condition, a bubble can freely cross over its own path and is thus more likely to remain in the cell, eventually leading to its destruction. This is evident in FIG. 6, where the cell moves

toward the active zone in the upper left corner but is destroyed due the absence of memorized flow.

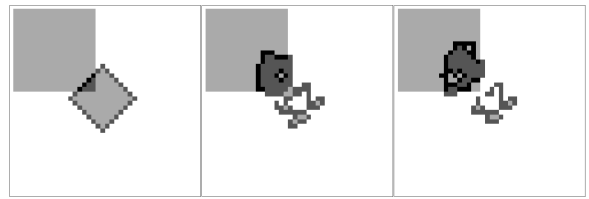


FIG. 6: Evolution of a cell without memorized flow in the presence of an active zone, defined as the shaded region in the upper left corner of the array. Time passes from left to right. The last image is obtained after 400 iterations.

## B. Adaptive networks

In the case of multiple active zones, there are several competing forces acting on the cell. Each active zone attracts the cell equally, yet the cell is also compelled to maintain its cohesion. Therefore, we observe a migration of its components to the active zones while maintaining a minimal connection between them, i.e., the cell forms an adaptive network between the food sources. Once two active zones are connected by a single path, this connection becomes stable, as there is no way for a bubble to deposit along its length and destroy it.

As can be seen in FIG. 7, where there are two active zones, the cell evolves to an approximate solution of the Steiner tree problem. We repeat the exercise with three and four active zones and obtain approximations to the corresponding Steiner tree solutions, as can be observed in FIG. 8 and 9. For comparison, we present in FIG. 10 the Steiner tree solutions for three and four vertices. The solution for two vertices is a single line between the vertices.

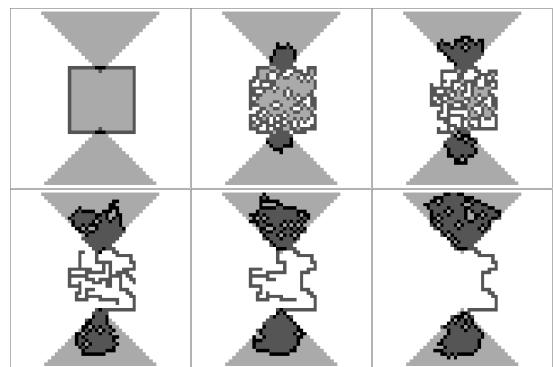


FIG. 7: Formation of an adaptive network between two active zones. Time moves from left to right and from top to bottom. The last image is obtained after 5900 iterations.

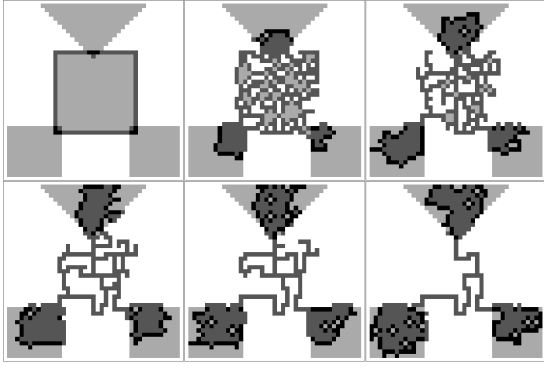


FIG. 8: Formation of an adaptive network between three active zones. Time moves from left to right and from top to bottom. The last image is obtained after 3400 iterations.

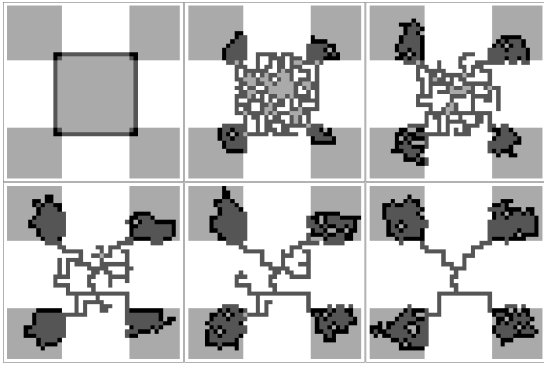


FIG. 9: Formation of an adaptive network between four active zones. Time moves from left to right and from top to bottom. The last image is obtained after 3300 iterations.

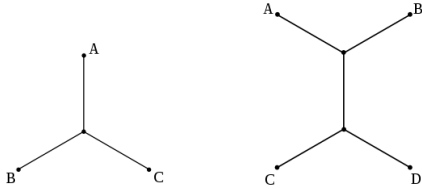


FIG. 10: Steiner tree solutions for three (left) and four (right) vertices.

If food sources are exhausted after an adaptive network has been formed, the cell is capable of recovering its original shape. We reproduce this property by iterating the

“eating 0” process on the 4-vertex adaptive network after removing the active zones, as can be observed in FIG. 11. It is clear that the cell slowly converges to an oval shape.

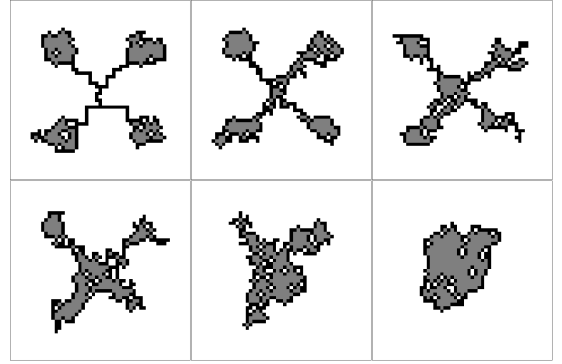


FIG. 11: Evolution of an adaptive network in the absence of active zones. Time moves from left to right and from top to bottom. The last image is obtained after 17200 iterations.

#### IV. CONCLUSIONS

The model used was capable of reproducing essential properties of unicellular systems such as *Physarum*. By introducing an element of adaptability, we were able to obtain both cell stability and the capacity for motion. Including minimal ingredients such as memorized flow and active zones, the model achieved the complex behaviour we aimed to emulate, namely the formation of robustly kept adaptive networks.

This toy model is thus able to replicate the characteristic intelligence of *Physarum*, which can be applied to more elaborate situations, such as the placement of more active zones in an asymmetric arrangement. One example is the application of the model to maze solving, as seen in [3].

We used the software *Mathematica* in order to take advantage of its visual display capabilities. However, the study of more complex arrangements of active zones would benefit from the use of a less computationally intensive programming language such as C++.

#### Acknowledgments

I would like to thank my colleagues Mariana Fernandes, Rita Franco and Martim Pardal for their support.

- 
- [1] M. Brazil, R. Graham, D. Thomas and M. Zachariasen, Arch. Hist. Exact Sci. **68** (2014) 327-354.
  - [2] I. Kunita, K. Yoshihara, A. Tero, K. Ito, C. Lee, M. Fricker and T. Nakagaki, PICT **6** (2013) 14-29.
  - [3] Y. Gunji, T. Shirakawa, T. Niizato and T. Haruna, J. Theor. Biol. **253** (2008) 659-667.
  - [4] D. Bottino, A. Mogilner, T. Roberts, M. Stewart and G. Oster, J. Cell. Sci. **115** (2002) 367-384.
  - [5] M. Karakozova, M. Kozak, C. Wong, A. Bailey, J. Yates III, A. Mogilner, H. Zebroski and A. Kashina, Science **313** (2006) 192-196.
  - [6] M. Zeleny, Int. J. Gen. Syst. **4** (1979) 13-28.